Transient Raman Observations of Heme Electronic and Vibrational Photodynamics in Deoxyhemoglobin

M. C. Simpson,*,†,‡ E. S. Peterson,§ C. F. Shannon,§ D. D. Eads,§ J. M. Friedman,§ C. M. Cheatum,† and M. R. Ondrias†

Contribution from the Department of Chemistry, University of New Mexico, Albuquerque, New Mexico 87135, and Department of Biophysics and Physiology, Albert Einstein College of Medicine, Bronx, New York 10461

Received April 11, 1996[⊗]

Abstract: Transient resonance Raman spectroscopy has been used to probe the vibrational dynamics of the heme active site of deoxyhemoglobin during photoexcitation. Near UV pulses of approximately 35 ps in duration were used to both excite the sample and generate resonance Raman spectra of the heme during its rapid electronic and vibrational relaxation. The behavior of the Stokes and anti-Stokes transitions as a function of incident laser flux directly reflects net heme vibrational populations and permits the isolation and characterization of ground and excited electronic state phenomena. Scattering from excited electronic states significantly influences the spectra only at the highest excitation fluxes used in this study. A simple model that accounts for the flux-dependent manifestations of the electronic and vibrational contributions to the heme transient resonance Raman spectra is discussed. In addition, the data presented here clearly show mode selectivity in the vibrational energy distribution associated with the ground electronic state. Stokes and anti-Stokes scattering from the prominent ν_4 and ν_7 modes reflect a heme with a non-Boltzmann vibrational population distribution, even at relatively modest excitation intensities. The ν_4 mode appears to act as a "bottleneck" vibrational state, while the ν_7 mode couples quite effectively to the bath degrees of freedom. The potential origins and ramifications of the creation and maintenance of such relatively long-lived, nonstatistical vibrational population distributions in the heme also are addressed.

Introduction

Energy redistribution dynamics can play a major role in directing photoinduced and collision-induced reactions in many small molecules.[1−4] In larger systems, specific molecular relaxation events immediately subsequent to activation may profoundly affect the initial branching ratios in complex reaction cascades and thereby influence events that occur on much longer time scales.[5] In molecules in the condensed phase, excess vibrational energy redistributes intramolecularly (IVR) and relaxes to the solvent (VR). The study of these two processes in large, solvated systems will lead to a general understanding of the mechanism(s) and functional implications of rapid vibrational energy dynamics. This manuscript reports studies of vibrational dynamics in the five-coordinate, high-spin Fe^{II} porphyrin active site of deoxyhemoglobin (dHb).

Metalloporphyrins comprise a diverse class of conjugated molecules that have large optical cross sections and a propensity for catalytic activity. In such systems it is likely that mode selective dissipation of excess vibrational energy plays a significant role in directing their chemical/biochemical reactions.[6,7] However, the vibrational motions critical for efficient function, and the means by which energy can be directed into them, remain to be determined. Elucidation of the mechanism(s) and pathway(s) of IVR and VR that accompany photoinduced electronic excitation and decay in metalloporphyrins is key to understanding the functional correlations between equilibrium and transient structures in metalloporphyrin-based enzymes. In addition, these findings will result in significant improvement in the use of metalloporphyrins as templates for the rational design of catalysts to carry out specific photodirected activities.

Five-coordinate Fe^{II} porphyrins are particularly good systems in which to examine vibrational dynamics using transient resonance Raman spectroscopy (TRRS). Photoexcitation of the heme active site generates two electronic excited states that rapidly undergo radiationless decay to deposit a large amount of excess vibrational energy in the ground electronic state.[8] The

* Author to whom correspondence should be addressed.
† University of New Mexico.
‡ Current address: Department of Chemistry, Case Western Reserve University, Cleveland, OH 44106.
§ Albert Einstein College of Medicine.
⊗ Abstract published in *Advance ACS Abstracts,* May 1, 1997.

(1) Butler, L. J.; Hintsa, E. J.; Shane, S. F.; Lee, Y. T. *J. Chem. Phys.* **1987**, *86*, 2051. Krajnovich, D.; Butler, L. J.; Lee, Y. T. *J. Chem. Phys.* **1984**, *81*, 3031.

(2) Metz, R. B.; Thoemke, J. D.; Pfeiffer, J. M.; Crim, F. F. *J. Chem. Phys.* **1993**, *99*, 1744. Sinha, A.; Hsiao, M. C.; Crim, F. F. *J. Chem. Phys.* **1990**, *92*, 6333. Sinha, A.; Hsiao, M. C.; Crim, F. F. *J. Chem. Phys.* **1991**, *94*, 4928. Bronikowski, M. J.; Simpson, W. R.; Zare, R. N. *J. Chem. Phys.* **1993**, *97*, 2197. Bronikowski, M. J.; Simpson, W. R.; Zare, R. N. *J. Chem. Phys.* **1993**, *97*, 2204.

(3) Reisler, H.; Keller, H.-M.; Schinke, R. *Comments At. Mol. Phys.* **1994**, *30*, 191.

(4) Zewail, A. H. *Phys. Today* **1980**, *Nov*, 27. Khundkar, L. R.; Zewail, A. H. *Ann. Rev. Phys. Chem.* **1990**, *41*, 15.

(5) Vos, M. H.; Jones, M. R.; Hunter, C. N.; Breton, J.; Martin, J. L. *Proc. Natl. Acad. Sci. U.S.A.* **1994**, *91*, 12701. Vos, M. H.; Rappaport, F.; Lambry, J.-C.; Breton, J.; Martin, J.-L. *Nature* **1993**, *363*, 320. Vos, M. H.; Jones, M. R.; Hunter, C. N.; Breton, J.; Lambry, J.-C.; Martin, J.-L. *Biochemistry* **1994**, *33*, 6750. Wynne, K.; Galli, C.; De Rege, P. J. F.; Therien, M. J.; Hochstrasser, R. M. *Springer Series in Chemical Physics;* Martin, J.-L., Migus, A., Mourou, G. A., Zewail, A. H., Eds.; 1993; Vol. 55, p 71. Stanley, R. J.; Boxer, S. G. *J. Phys. Chem.* **1995**, *99*, 859. Zhu, L.; Wang, W.; Sage, J. T.; Champion, P. M. *J. Raman Spectrosc.* **1995**, *26*, 527. Zhu, L.; Sage, J. T.; Champion, P. M. *Science* **1994**, *266*, 629. Wang, Q.; Schoenlein, R. W.; Peteanu, L. A.; Mathies, R. A.; Shank, C. V. *Science* **1994**, *266*, 422.

(6) Gu, Y.; Li, P.; Sage, T.; Champion, P. M. *J. Am. Chem. Soc.* **1993**, *115*, 4993.

(7) Miller, D. R. J. *Ann. Rev. Phys. Chem.* **1990**, *42*, 589. Ansari, A.; Berendzen, J.; Browne, S. F.; Frauenfelder, H.; Eben, I. E. T.; Sauke, T. B.; Shyamsunder, E.; Young, R. D. *Proc. Natl. Acad. Sci. U.S.A.* **1985**, *82*, 5000. Elber, R.; Karplus, M. *Science* **1987**, *235*, 218.

(8) Petrich, J. W.; Poyart, C.; Martin, J. L. *Biochemistry* **1988**, *27*, 4049. Petrich, J. W.; Martin, J. L. *Chem. Phys.* **1989**, *131*, 31.

S0002-7863(96)01198-5 CCC: $14.00

system then returns to thermal equilibrium via IVR among heme "normal" modes and VR to the protein/solvent. The large heme optical cross section allows this stimulation and recovery to be monitored by the single-pulse TRRS method. The ratio of the integrated anti-Stokes and Stokes scattering, corrected to first order for cross section[9] and reabsorption differences, yields direct information about relative vibrational populations. In TRRS, the dependence of this ratio and of the band characteristics upon laser flux reveals mode selective IVR/VR behavior by taking advantage of the ability of relatively long, high-intensity laser pulses to generate populations of transient species whose lifetimes are shorter than the pulse width.[13,15−17] Hence, the picosecond scale processes of IVR and VR can be studied with 10 ns pulses. This approach has demonstrated that a steady-state non-Boltzmann vibrational energy distribution can be established and measured in dHb[15] and model iron porphyrins.[15−17] This mode selective behavior appears intrinsic to the metalloporphyrin structure and may affect metalloporphyrin function.[15−17]

Vibrational dynamics in metalloporphyrins are not yet well understood. Evidence for IVR has been found in fluorescence excitation spectra of a few jet-cooled porphyrins.[10] Spectral congestion and the independence of the fluorescence lifetime upon degree of vibrational excitation have been interpreted as indirect evidence for efficient IVR in the metalloporphyrin S_1 excited state. A few studies have been carried out upon vibrational energy dynamics in solvated metalloporphyrins as well. Previous transient and time-resolved studies used femtosecond, picosecond, and nanosecond laser pulses to interrogate the internal dynamics of photoexcited hemes in proteins.[8,11−17] Unfortunately, the interpretation of these results is quite model-dependent. The results presented in this paper will help resolve several issues.

The importance of mode selective vibrational energy dynamics and the presence of a relatively long-lived, low-lying electronic excited state are currently topics of debate. The electronic behavior of dHb subsequent to photoexcitation has been fairly well characterized. Petrich and others[8,11] have used femtosecond transient absorbance and resonance Raman spectroscopy to determine that photoexcitation into either the Soret or Q-band generates at least two transient electronic states, Hb_I* and Hb_{II}*, that decay with lifetimes of ∼300 fs and ∼3 ps, respectively. The Raman scattering from the longer-lived species exhibits bleaching of the major vibrational transitions and shifting of the ν_4 Stokes line to lower frequency by as much as 8 cm^{-1}.[11] The decay of the Hb_I* and Hb_{II}* states generates a vibrationally hot ground state.

Other groups have studied the vibronic dynamics of this system as well. Lingle et al. monitored Stokes and anti-Stokes scattering from photoexcited dHb using time-resolved resonance Raman spectroscopy (8 ps pulses).[12] They observed Stokes saturation and increased anti-Stokes scattering that decayed on a ∼10 ps time scale and concluded that their results could be explained only in terms of the vibrational relaxation of a thermally excited ground state heme. It was asserted that all thermalization and electronic decay processes occurred more rapidly than could be measured, producing a heme with a Boltzmann temperature higher than that of the bath. However, this interpretation relied upon a physically unrealistic two-level model and assumed an "instantaneous" equipartition of vibrational energy. A study of the low-frequency (<800 cm^{-1}) modes of dHb using ∼30 ps pulses by Ondrias, Friedman, and co-workers revealed that those modes were not vibrationally excited on the experimental time scale.[14]

Ondrias and co-workers used nanosecond TRRS to study heme photophysics in dHb and model hemes.[15−17] They observed an abnormally intense, flux-dependent anti-Stokes scattering that was significantly more prominent for the ν_4 mode than for other vibrations. This behavior was interpreted in terms of IVR and VR associated with a nonthermal vibrationally excited ground state. The assignment of the results to vibrational rather than to electronic excited state behavior was based upon several observations: (1) no evidence for saturation of the Stokes transitions was found, (2) all bands were fit well with single Lorentzian lines, (3) the Stokes ν_4 band did not show the shift to lower frequency characteristic of known dHb electronic excited states,[11] and (4) the integrated anti-Stokes signal intensity for ν_4 increased dramatically and this band shifted to lower frequency with increasing laser flux. Simple lifetime calculations determined that these results were reasonable for the laser fluxes involved and for acceptable vibrational decay rates.

TRR spectroscopy with nanosecond pulses also was used by Champion and co-workers to examine the photoresponse of dHb.[13] These researchers employed laser pulses that were greater than 10-fold more intense than those used by Simpson et al.[15−17] In addition to the mode selective, flux-dependent increase in anti-Stokes scattering, saturation of the ν_4 Stokes line and the presence of a transient band to lower frequency underlying ν_4 also were found. The flux-dependent results were interpreted in terms of an electronic excited state with a 2 ps lifetime, an anomalously large anti-Stokes cross section for ν_4, and a dipole-allowed absorption at/near that of the ground state. Asymmetric broadening of ν_4 has also been attributed to Rabi broadening effects.[14b] In light of subsequent experimental data, this interpretation is not likely to be correct,[13] and will not be discussed further here. Thus, similar spectroscopic observations have resulted in significantly different explanations of the underlying photoinduced dynamics that invoke varying degrees of electronic and/or vibrational excitation.

The present study extends the previous nanosecond transient investigations into the picosecond domain. Here, we report TRR spectroscopic measurements of dHb using 35 ps, Soret-resonant

(9) Hizhnyakov, V.; Tehver, I. *Phys. Status Solidi* **1967**, *21*, 755. Tonks, D. L.; Page, J. B. *Chem. Phys. Lett.* **1979**, *66*, 449. Hassing, S.; Mortensen, O. S. *J. Chem. Phys.* **1980**, *73*, 1078. Stallard, B. R.; Champion, P. M.; Callis, P. R.; Albrecht, A. C. *J. Chem. Phys.* **1983**, *78*, 712. Bangcharoenpaurpong, O.; Shomaker, K. T.; Champion, P. M. *J. Am. Chem. Soc.* **1984**, *106*, 5688. Schomaker, K. T.; Champion, P. M. *J. Chem. Phys.* **1989**, *90*, 5982.

(10) Even, U.; Magen, Y.; Jortner, J.; Levanon, H. *J. Chem. Phys.* **1982**, *76*, 5684. Even, U.; Magen, J.; Jortner, J.; Friedman, J. M.; Levanon, H. *J. Chem. Phys.* **1982**, *77*, 4374. Even, U.; Magen, J.; Jortner, J.; Friedman, J. M. *J. Chem. Phys.* **1982**, *77*, 4384. Even, U.; Jortner, J. *J. Chem. Phys.* **1982**, *77*, 4391. Fitch, P. S. H.; Wharton, L.; Levy, D. H. *J. Chem. Phys.* **1979**, *70*, 2018. Fitch, P. S. H.; Haynam, C. A.; Levy, D. H. *J. Chem. Phys.* **1981**, *74*, 6612.

(11) Franzen, S.; Bohn, B.; Poyart, C.; Martin, J. L. *Biochemistry* **1995**, *34*, 1224.

(12) Lingle, R., Jr.; Xu, X.; Zhu, H.; Yu, S.-C.; Hopkins, J. B. *J. Phys. Chem.* **1991**, *95*, 9320. Lingle, R., Jr.; Xu, X.; Zhu, H.; Yu, S.-C.; Hopkins, J. B. *J. Am. Chem. Soc.* **1991**, *113*, 3992.

(13) Li, P.; Sage, J. T.; Champion, P. M. *J. Chem. Phys.* **1992**, *97*, 3214.

(14) (a) Alden, R. G.; Chavez, M. D.; Courtney, S. H.; Friedman, J. M.; Ondrias, M. R. *J. Am. Chem. Soc.* **1990**, *112*, 3241. Alden, R. G.; Schneebeck, M. C.; Ondrias, M. R.; Courtney, S. H.; Friedman, J. M. *J. Raman Spectros.* **1992**, *23*, 569. (b) Alden, R. G.; Ondrias, M. R.; Courtney, S. H.; Findsen, E. W.; Friedman, J. M. *J. Phys. Chem.* **1990**, *94*, 85.

(15) Schneebeck (Simpson), M. C.; Vigil, L. E.; Ondrias, M. R. *Chem. Phys. Lett.* **1993**, *215*, 251.

(16) (a) Simpson, M. C. Ph.D. Dissertation, University of New Mexico School of Medicine, 1994. (b) Simpson, M. C.; Millett, F.; Pan, L. P.; Larsen, R. W.; Hobbs, J. D.; Fan, B.; Ondrias, M. R. *Biochemistry* **1996**, *35*, 10019.

(17) Cheatum, C. M.; Ondrias, M. R.; Simpson, M. C. *Proceedings of the Seventh International Conference on Time Resolved Vibrational Spectroscopy*, 1995; abstract P8.

(436 nm) laser pulses. We also discuss a model that places these results in the context of previous investigations by ourselves and others and qualitatively accounts for observed electronic and vibrational behavior of photoexcited metalloporphyrins over a wide range of excitation fluences and time scales. The saturation of the resonance Raman spectrum observed by Champion and co-workers[13] and Lingle et al.[12] is entirely consistent with the photodynamics of Hb_I* and Hb_{II}*. On the other hand, the anti-Stokes scattering increase and band broadening observed in the absence of saturation effects by Simpson et al.[15−17] and superimposed upon the saturation in other experiments[12,13] can be attributed to vibrational excitation associated with the ground electronic state of the heme. The origins and significance of the distinct mode specificity observed in the ground state vibrational energy distribution also are addressed.

Experimental Methods

Human hemoglobin was purified from whole blood as previously described.[18] Samples of ∼200 μM dHb in 0.1 M Tris, pH 8.0, were prepared by anaerobic reduction with a small excess of solid sodium dithionite. Samples were held in an anaerobic quartz cuvette, with a temperature maintained at 20 °C. Evidence of laser induced sample degradation was monitored by comparison of electronic absorption spectra taken before and after Raman spectroscopy.

Transient resonance Raman spectra were measured as follows. The second harmonic of a Continuum model PY61C-20 active/passive mode-locked Nd:YAG laser (20 Hz, 35 ps, av pulse power = 30−35 mJ) was H_2-Raman shifted (460 psi of H_2) to generate 436 nm pulses. Flux was attenuated using neutral density filters. The power of a fraction of the beam was continually monitored during spectral acquisition. Raman scattering was collected in a backscattered geometry (∼155°) with a 2 inch, F2.5 Triplet (CVI) lens. A holographic filter (Kaiser Optical Systems, 442 nm) was angle-tuned to reject Rayleigh scattering. The collection optics were *f*-matched to the spectrometer and included a polarization scrambler (Karl Lambrecht, Inc.). The collected light was dispersed using an Instruments SA model HR 640 single-grating (1800 grooves/mm, entrance slit = 150 μm × 5 mm) spectrometer and detected with an Instruments SA Spectraview-2D liquid nitrogen cooled CCD array. Lamp spectra calibrated the wavelength axis and corrected for λ-dependent transmission of the holographic filter. Laser flux at the sample was calculated from the laser intensity, the repetition rate, and the area of the laser spot at the sample. This area was measured by translating a metal shim across the spot at the sample position.

Stokes and anti-Stokes peaks were decomposed into Lorentzian line shapes with either a quadratic or a linear baseline function. Spectra were fit using both a commercially available package (Peakfit, Jandel Scientific Software, AISN Software Inc.) and a curve-fitting program based upon the Levenberg−Marquardt nonlinear least squares method.[16a] The noncommercial program has a number of advantages for fitting data of the type encountered in this study: the step size taken during minimization can be varied as needed, the minimization process is monitored at each step, and the total intensities of signal and background are irrelevant. These features provide more control over the fitting process, thereby allowing accurate fitting of low-intensity peaks on low and high backgrounds. The ability of the noncommercial routine to fit real and simulated spectra with accuracy has been tested as a function of the initial parameter guesses (i.e., peak height, width, and position), signal-to-noise ratios, peak separations, and peak relative intensities.[16b] Most of the spectra reported here consist of isolated, well-separated peaks. For the major Stokes and anti-Stokes transitions, the position-fitting errors are smaller than the detection limit of ±0.5 cm^{-1}. The only band for which this error may be greater is the minor transient component that underlies the ν_4 band at the highest flux employed. For more details concerning the accuracy of the fitting process used, see the Supporting Information to ref 16b.

(18) Antonini, E.; Brunori, M. *Hemoglobin and Myoglobin and their Reactions with Ligands*; North-Holland: Amsterdam, The Netherlands, 1971; pp 1−3.

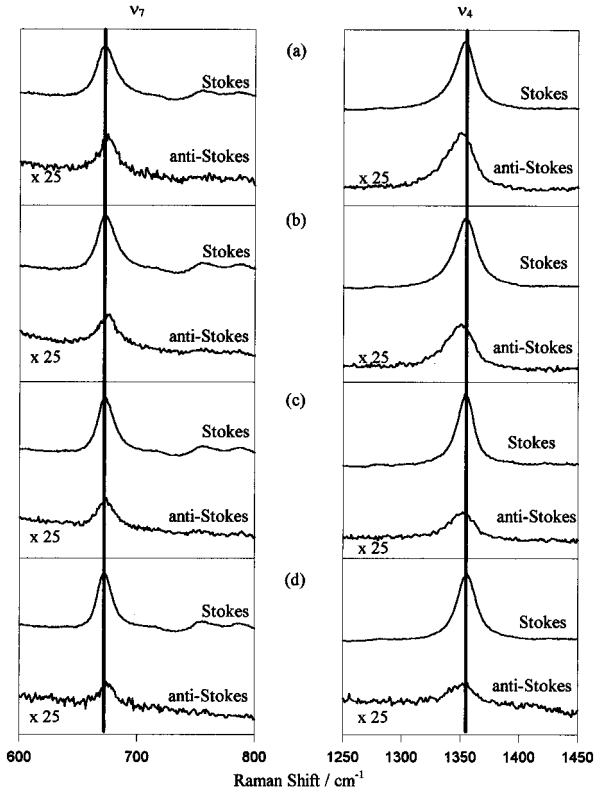

Figure 1. Transient resonance Raman spectra of the ν_4 and ν_7 regions of the deoxyhemoglobin spectrum as a function of incident laser flux using 35 ps pulses (λ_{ex} = 436 nm). See Experimental Methods for details concerning the sample conditions and the spectroscopic apparatus: (a) 12 × 10^8 W/cm^2; (b) 6 × 10^8 W/cm^2; (c) 3 × 10^8 W/cm^2; and (d) 1.5 × 10^8 W/cm^2.

Anti-Stokes/Stokes area ratios were corrected for cross section differences by using a previously published method that takes advantage of the optical theorem and the Kramers−Kronig transform[9] and for reabsorption differences using a straightforward integration scheme.[16a]

Results

The TRR spectrum of dHb was measured using 35 ps incident laser pulses with fluxes ranging from 1.5 × 10^8 to 12 × 10^8 W/cm^2 at 436 nm. Band widths, positions, and intensities were examined as functions of incident flux. The pulses were not sufficiently long to allow the system to reach a true steady state. Hence, the picosecond data are somewhat noisier that their nanosecond counterparts. The flux dependence of anti-Stokes and Stokes scattering from dHb using 35 ps wide pulses are summarized in Figures 1−3 and Table 1.

Several observations concerning the response of the dHb to increased laser flux can be made. First, the relative anti-Stokes transition intensities changed with incident laser flux (Figure 1, Table 1). The integrated area of anti-Stokes scattering increased relative to that of Stokes scattering for all modes, although the magnitude of this effect was mode-dependent. For example, over the incident flux range of 3 × 10^8 to 12 × 10^8 W/cm^2, this ratio increased by a factor of about 2.6 for ν_4 and of 1.4 for ν_7. First-order corrections can be made to the anti-Stokes/Stokes area ratios to account for the differences in reabsorption and resonance Raman cross sections using a method that applies the optical theorem and the Kramers−Kronig transform.[9,16a] The heme "temperatures" indicated by these corrected ratios were found to be from 580 to 820 K for ν_4 and from 260 to 310 K for ν_7 over the fluxes employed (Table 1). Other modes, for example ν_3, also exhibited elevated heme "temperatures"; however, the inferior signal-to-noise ratio of

Table 1. Picosecond TRR Spectroscopy of Deoxyhemoglobin Curve Fit Results[a]

	ν_4							ν_7						
flux (W/cm$^{2)}$	ω_S	Γ_S	ω_{aS}	Γ_{aS}	ratio (%)	T_B (K)	T_C (K)	ω_S	Γ_S	ω_{aS}	Γ_{aS}	ratio (%)	T_B (K)	T_C (K)
12×10^8	1354	18	1349	29	7.4	750	820	672	19	675	19	2.9	270	310
6×10^8	1354	22	1350	29	3.8	600	630	673	19	675	21	2.6	270	300
3×10^8	1354	17	1351	26	2.8	550	580	673	17	674	18	2.1	250	280
1.5×10^8	1355	20						672	15	675	15	1.5	230	260

[a] Bands were fit with Lorentzian line shapes. Γ and ω are full width at half maximal intensity and peak positions in cm^{-1}, respectively. The "S" and "aS" subscripts refer to Stokes and anti-Stokes scattering, respectively. Ratio = the anti-Stokes integrated intensity/the Stokes integrated intensity, corrected for λ-dependent transmission by the holographic filter. T_B = the Boltzmann predicted temperature of the heme reflected by the anti-Stokes/Stokes area ratio. T_C = the temperature of the heme reflected by the anti-Stokes/Stokes area ratio approximately corrected for reabsorption and cross section difference.[9]

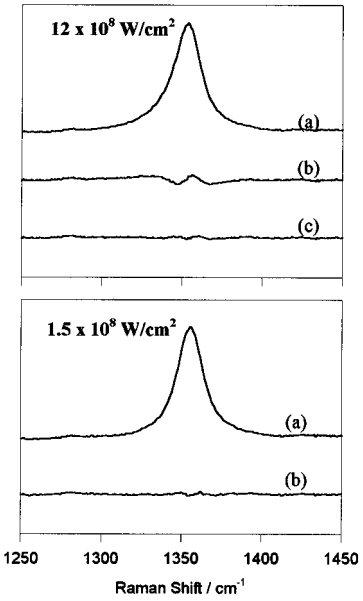

Figure 2. Stokes spectra of the ν_4 region of deoxyhemoglobin at the lowest (1.5×10^8 W/cm^2) and highest (12×10^8 W/cm^2) incident fluxes. Same data acquisition parameters and sample condition as Figure 1: (a) experimental data; (b) and (c) difference between experimental data and curve fit resulting from fitting the ν_4 band with a single peak (b) or with two peaks (c). Difference = data − fit.

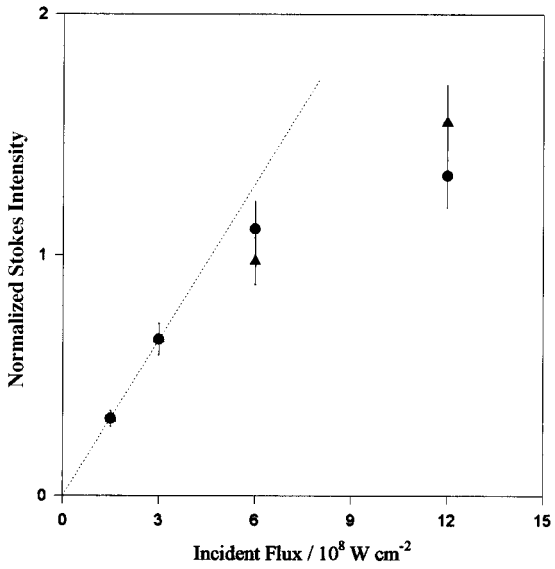

Figure 3. The integrated area of the ν_4 (solid circles) and ν_7 (solid triangles) Stokes bands as a function of incident laser flux. The total integrated flux of ν_7 was normalized to that of ν_4 by averaging the $I_{\nu4}/I_{\nu7}$ ratio for all incident laser fluxes (average = 1.662), and then multiplying the integrated areas of ν_7 by this average. The straight line indicates the linear regression fit through the origin (0 flux, 0 signal) and the first two data points of both bands (fluxes 1.5×10^8 and 3×10^8) ($r^2 > 0.9999$). The error bars mark the error estimate of ±10%.

these much weaker bands precluded quantitation using the current data set.

The line width and position of the anti-Stokes ν_7 transition were found to be very similar to those of the ν_7 Stokes band at all flux levels. No systematic changes in Stokes and anti-Stokes ν_7 positions were observed, although both line widths increased slightly with incident flux. In contrast, the line width and position of the ν_4 anti-Stokes band differed significantly from that of the ν_4 Stokes transition at each incident flux value. The anti-Stokes ν_4 line consistently appeared 3−5 cm^{-1} lower in energy and ∼10 cm^{-1} broader than its corresponding Stokes transition. Neither the ν_4 Stokes nor the ν_4 anti-Stokes bands exhibited a systematic line width change in response to increased laser flux. However, although the Stokes ν_4 band position remains relatively constant, the anti-Stokes position shifts to lower frequency. This observation is based upon the fact that, over the interval of 3×10^8 to 12×10^8 W/cm^2, the variations seen in the positions of the ν_4 Stokes, ν_7 Stokes, and ν_7 anti-Stokes transitions were not systematic and were within the detection uncertainty limits of ±0.5 cm^{-1}. On the other hand, the ν_4 anti-Stokes band shifts systematically by 2 cm^{-1} from 1351 to 1349 cm^{-1} across the same flux range.

Finally, at the highest incident flux, 12×10^8 W/cm^2, it was necessary to fit the Stokes ν_4 band with an additional component (Figure 2). That this second band was required only at the highest flux can be seen in the single-band residuals. These residuals were calculated by fitting the Stokes spectra with a single Lorentzian for ν_4 and subtracting the total fit from the raw data. Curve-fitting procedures revealed that this second component appeared at about 1345 cm^{-1} with a full width at half maximum intensity of approximately 35 cm^{-1}. In addition, strong evidence of saturation of Stokes transitions was found at the highest flux (Figure 3). At incident power densities of less than 6×10^8 W/cm^2, the relationship between the integrated ν_7 and ν_4 Stokes intensities and the incident laser flux was determined to be linear ($r^2 > 0.9999$). A slight deviation from this linearity appeared at 6×10^8 W/cm^2. However, with 12×10^8 W/cm^2 incident flux, clear deviation from this linear behavior was obvious.

Discussion

This manuscript reports results of TRR studies of dHb using 35 ps pulses. In transient (single-pulse) spectroscopy, the molecule is excited and probed within a single pulse. As the incident photon density is changed, the average "time interval" between photoexcitation and probe events varies. Thus, the

average delay within a given pulse between the "pump photon" and "probe photon" can be controlled with the laser flux. Differences in transient spectra as a function of laser flux indicate the presence of evolving photoexcited species. In this manner, specific details of heme photophysical processes that occur on time scales that are comparable to or more rapid than the temporal pulse width can be studied.[13,15−17] Discerning the origin(s) of the observed flux-dependent spectral changes of the heme resonance Raman spectrum is the subject of the remainder of this report.

A Model for Heme Photophysics in Deoxyhemoglobin. Three independent groups have observed qualitatively similar spectroscopic results upon photoexcitation of the heme in dHb. However, the interpretations of these phenomena vary. An electronic excited state,[13] and both thermal[12] and nonthermal[15−17] vibrational energy distributions associated with the ground electronic state all have been invoked to explain the experimental data.

The picosecond TRRS data provide a basis for a simple kinetic model that connects the observations of the Hopkins, Champion, Friedman, and Ondrias groups within the context of the established electronic photodynamic behavior of this system (see Introduction). The incident laser fluxes used here are particularly relevant for resolving the apparent conflict. Only at the highest incident laser flux in the picosecond TRR experiments was clear evidence for an electronic excited state found (Figures 2 and 3). The position of the transient ν_4 Stokes band ($\sim$1345 cm^{-1}) is consistent with its assignment to Hb_{II}^*. In contrast, under conditions of significantly lower incident flux, the anti-Stokes signal was still abnormally intense, although the Stokes line was fit well with a single Lorentzian line shape. In addition, a linear dependence of Stokes intensity upon incident flux was observed at low laser powers. It is important to note that ν_4 and ν_7 exhibit indistinguishable saturation behavior. Thus, the flux-dependent, mode selective anti-Stokes behavior can be temporally separated from the ν_4 Stokes asymmetric broadening and the mode independent Stokes saturation. The manifestations of the electronic bottleneck Hb_{II}* appear to complicate the nanosecond and picosecond TRR observations only at incident laser fluxes in the $>10^9$ W/cm^2 range, where the earlier events in the photodynamics are probed. The anomalous anti-Stokes behavior therefore appears to originate from the later events associated with excited vibrational levels of the ground electronic state.

The simple photophysical cycle depicted in Figure 4 has been developed to explain the major features of photoinduced dHb behavior. The specific concern is whether it is reasonable to conclude that the vibrational excitation in the ground state can be probed in the absence of significant complications arising from electronic excitation. Therefore, this model does not address the mode selectivity of IVR and VR. Rather, these processes are folded into a global vibrational excitation that decays with a single characteristic time constant.

The cycle runs as follows. Upon photoexcitation, the heme immediately (<50 fs) evolves to either an Hb_I* or an Hb_{II}* electronic excited state. The initial ratio of these two states is assumed to be 1.0 for the test calculations, based upon comparison to deoxymyoglobin results, in which it was determined that about 65% of photoexcited deoxymyoglobin returns to the ground electronic state via Hb_I*.[8] The 1:1 ratio chosen here results in a more stringent test of the model.

The vibrational relaxation of these electronic excited states will occur concurrently with their electronic relaxation. However, even in our highest flux experiments, the population of the electronic excited states appears to be quite small, and we

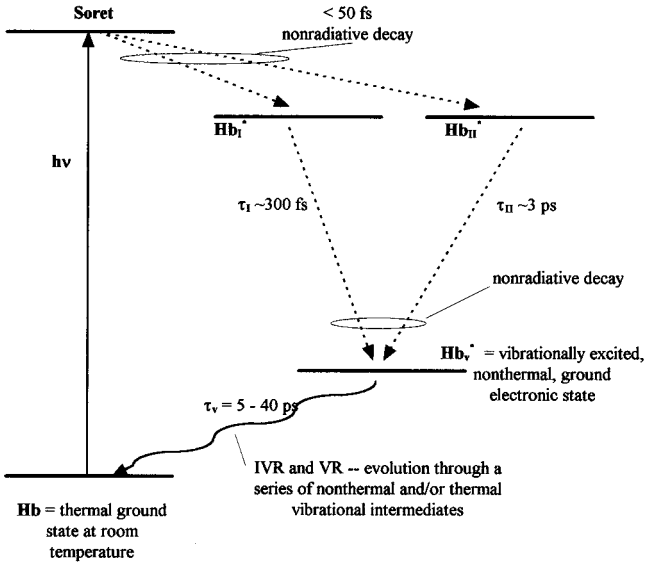

Figure 4. Kinetic model for the initial response of deoxyhemoglobin to photoexcitation based upon data presented in refs 8, 11, 14−17, abd 19−21.

do not detect anti-Stokes scattering from vibrationally excited Hb_I* and Hb_{II}*. Anti-Stokes Raman lines broaden symmetrically and shift smoothly to lower frequency as incident flux is increased, in the absence of any evidence for additional components. Notably, the small transient band in the ν_4 Stokes spectrum assigned to electronic excited state(s) is simply not observed in the anti-Stokes spectrum. Our inability to directly monitor anti-Stokes signals from this small population of the electronic excited state is entirely reasonable, given the very small contribution of electronic excited state scattering to the highest flux Stokes signal, the relative intensities of Stokes and anti-Stokes scattering, and the typical signal-to-noise of anti-Stokes data. Hence, saturation of the anti-Stokes signal with incident laser flux due to ground state depletion would be the only indication of excited electronic state population we could reasonably expect to observe. This very minor and indirect manifestation of excited electronic state vibrational population is overwhelmed by the dramatic, nonlinear, mode selective increases in anti-Stokes intensity that derive from vibrational excitation of the ground state. We cannot, at this point, identify the effects of this minor component, much less address any issues concerning vibrational relaxation of the electronic excited states. Given the above issues, we have reasonably omitted specific reference to excited electronic state vibrational relaxation within the kinetic model and assigned a single nonradiative decay rate constant to each electronic excited state. This approximation will not change the conclusions drawn from examination of the kinetic model.

The lifetime of Hb_I* is 300 fs in accordance with Petrich et al.[8] A lifetime of 3.0 ps is chosen for Hb_{II}* and is in good agreement with measurements by Petrich et al.,[8] Franzen et al.,[11] and Champion et al.[13] Both of these states decay nonradiatively to produce a vibrationally excited ground electronic state that relaxes intra- and intermolecularly. The single, general lifetime of this vibrational excitation is estimated to be 5−40 ps. This estimate is based upon measurements in other molecules,[19] calculations by Henry et al.,[20] photoacoustic grating results of Miller and co-workers,[21] the nanosecond TRR measurements by Schneebeck/Simpson et al.,[15−17] and the data presented in this manuscript. The cycle thus returns the heme to its electronic ground state with a thermal vibrational energy distribution characteristic of the temperature of the environment (heat bath).

From this model, the following simple expressions for the components of interest can be written:

$$[\mathrm{Hb_I}^*] = [\mathrm{Hb_I}^*]_0 e^{-k_\mathrm{I} t} \quad (1)$$

$$[\mathrm{Hb_{II}}^*] = [\mathrm{Hb_{II}}^*]_0 e^{-k_\mathrm{II} t} \quad (2)$$

$$[\mathrm{Hb(v^*)}] = \frac{[\mathrm{Hb_I}^*]_0 k_\mathrm{I}}{k_\mathrm{I} - k_\mathrm{v}}\{e^{-k_\mathrm{v} t} - e^{-k_\mathrm{I} t}\} + \frac{[\mathrm{Hb_{II}}^*]_0 k_\mathrm{II}}{k_\mathrm{II} - k_\mathrm{v}}\{e^{-k_\mathrm{v} t} - e^{-k_\mathrm{II} t}\} \quad (3)$$

The species and rate constants are defined in Figure 4.

Representative population analyses with global lifetimes for the vibrational excitation of 5, 10, 20, and 40 ps are presented in Figure 5. The model presented here readily accounts for the observed photophysical behavior of the heme in dHb. Even at the shortest vibrational state lifetime, $\tau_\mathrm{v} = 5$ ps, a considerable population of vibrationally excited heme persists beyond the point at which $\mathrm{Hb_{II}}^*$ ($\tau = 3$ ps) has decayed completely. In addition, at all τ_v employed in these simulations, the electronic excitation temporally overlaps vibrational excitation. Although the degree to which this overlap occurs will depend upon the ratio of initial ($t = 0$) concentrations of $\mathrm{Hb_I}^*$ and $\mathrm{Hb_{II}}^*$, it is apparent that the two processes will always coincide.

Within the context of the above model, it becomes clear that the Champion, Hopkins, Friedman, and Ondrias groups have simply probed different regions of the net vibronic decay processes. The data of Li et al.[13] and Lingle et al.[12] arose from a regime where significant electronic excited state persists along with a vibrationally excited ground state. Hence, they found both the anomalous anti-Stokes intensities and the Stokes saturation phenomenon. Simpson et al.[15−17] examined the vibrationally excited ground state in the nanosecond TRR studies and at the lower fluxes in the picosecond TRR studies reported here. In the highest flux picosecond TRR spectra, however, electronic excited state behavior contributed. The results of the current picosecond TRR studies thus bridge the results obtained by Champion, Hopkins, Friedman, Ondrias, and their co-workers and provide direct evidence for the assignment of the anti-Stokes behavior to ground electronic state vibrational energy dynamics.

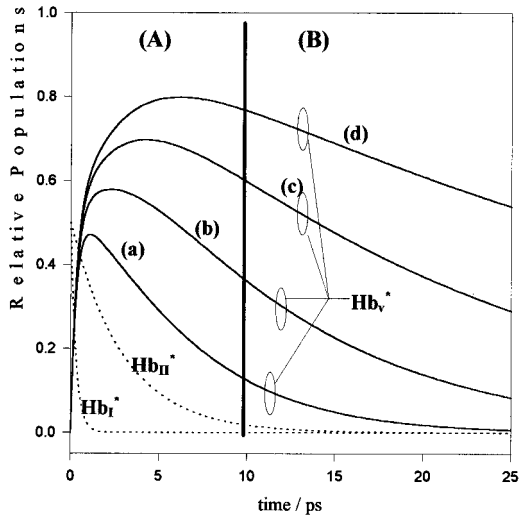

Figure 5. Calculations of the populations of $\mathrm{Hb_I}^*$, $\mathrm{Hb_{II}}^*$, and $\mathrm{Hb_v}^*$ as a function of time. These are calculated using eqs 1−3 in the text. Time constants of $\tau_\mathrm{I} = 1/k_\mathrm{I} = 300$ fs and $\tau_\mathrm{II} = 1/k_\mathrm{II} = 3$ ps were used. $\tau_\mathrm{v} = 1/k_\mathrm{v}$ was varied: (a) 5 ps; (b) 10 ps; (c) 20 ps; (d) 40 ps. Region A is dominated by electronic excited state dynamics. This region is probed by the Champion,[13] Hopkins,[12] and Martin[8] groups. Saturation and asymmetric broadening of Stokes transitions are seen, in addition to increased anti-Stokes scattering from the vibrationally excited ground electronic state. Region B is dominated by vibrational excited state dynamics. This region is probed by Simpson et al. in previous work[15−17] and in the lower flux picosecond TRR studies reported here. Increased anti-Stokes scattering is observed in the absence of saturation and asymmetric broadening of Stokes lines.

A Non-Boltzmann Vibrational Energy Distribution in Photoexcited Deoxyhemoglobin. The model above assures that it is reasonable to interpret the mode selective, flux-dependent Raman-scattering behavior observed in the nanosecond and picosecond TRR spectra of deoxyhemoglobin in terms of vibrational excitation of ground electronic state. The mode selectivity of vibrational energy dynamics in this large molecule in the condensed phase can now be explored in the absence of complications arising from population of bottleneck electronic excited states.

Excited vibrational states of molecules in solution decay with lifetimes from subpicosecond to nearly a nanosecond.[19] Despite this diversity, a rough sketch of vibrational dynamics in solution emerges. The first step usually involves rapid (<2 ps) intramolecular redistribution among isoenergetic vibrations.[19a−e] For example, excitation of one CH stretch often leads to "immediate" population of other CH stretch modes.[19a,b] This subset of states can act as a bottleneck, with a lifetime of ten or hundreds of picoseconds. In the second stage, other modes directly or indirectly gain population.[19a,d,e] In nitromethane/methanol complexes, excitation of the OH stretch appears first in the methanol CH stretches and bends and then in the nitromethane NO_2 stretch.[19e] Eventually (often tens to hundreds of picoseconds), the molecule reaches thermal equilibrium with its local environment.

Localization of vibrational energy in a subset of the available degrees of freedom in photoexcited, solvated hemes has been previously observed using nanosecond TRRS.[15−17] In these experiments, the ratio of anti-Stokes to Stokes scattering was used to determine if the heme was at thermal equilibrium during

(19) (a) Fendt, A.; Fischer, S. F.; Kaiser, W. *Chem. Phys.* **1981**, *57*, 55. Spanner, K.; Laubereau, A.; Kaiser, W. *Chem. Phys. Lett.* **1976**, *44*, 88. Graener, H.; Ye, T. Q.; Laubereau, A. *J. Phys. Chem.* **1989**, *93*, 7044. Gottfried, N. H.; Kaiser, W. *Chem. Phys. Lett.* **1983**, *101*, 331. (b) Zinth, W.; Kolmeder, C.; Benna, B.; Irens-Defrigger, A.; Fischer, S. F.; Kaiser, W. *J. Chem. Phys.* **1983**, *78*, 3916. Scherer, P. O. J.; Seilmeier, A.; Kaiser, W. *J. Chem. Phys.* **1985**, *83*, 3948. Seilmeier, A.; Scherer, P. O. J.; Kaiser, W. *Chem. Phys. Lett.* **1984**, *105*, 140. Chen, S.; Hong, X.; Hill, J. R.; Dlott, D. D. *J. Phys. Chem.* **1995**, *99*, 4525. (c) Arrivo, S. H.; Dougherty, T. P.; Grubbs, W. T.; Heilweil, E. J. *Chem. Phys. Lett.* **1995**, *235*, 247. Tokmakoff, A.; Sauter, B.; Kwok, A. S.; Fayer, M. D. *Chem. Phys. Lett.* **1994**, *221*, 412. (d) Kolmeder, C.; Zinth, W.; Kaiser, W. *Chem. Phys. Lett.* **1982**, *91*, 323. Laubereau, A.; von der Linde, D.; Kaiser, W. *Phys. Rev. Lett.* **1972**, *28*, 1162. Graener, H. *Chem. Phys. Lett.* **1990**, *165*, 110. Ambroseo, J. R.; Hochstrasser, R. M. *J. Chem. Phys.* **1988**, *89*, 5956. Hubner, H.-J.; Worner, M.; Kaiser, W. *Chem. Phys. Lett.* **1991**, *182*, 315. (e) Hong, X.; Chen. S.; Dlott, D. D. *J. Phys. Chem.* **1995**, *99*, 9102. (f) Heilweil, E. J.; Cavanagh, R. R.; Stephenson, J. C. *Chem. Phys. Lett.* **1987**, *134*, 181. Tokmakoff, A.; Sauter, B.; Fayer, M. D. *J. Chem. Phys.* **1994**, *100*, 9035. Moore, P.; Tokmakoff, A.; Keyes, T.; Fayer, M. D. *J. Chem. Phys.* **1995**, *103*, 3325. Kenkre, V. M.; Tokmakoff, A.; Fayer, M. D. *J. Chem. Phys.* **1994**, *101*, 10618. Doany, F. E.; Greene, B. I.; Hochstrasser, R. M. *Chem. Phys. Lett.* **1980**, *75*, 206. Fleming, G. R. *Ann. Rev. Phys. Chem.* **1986**, *3*, 81. Gottfried, N. H.; Seilmeier, A.; Kaiser, W. *Chem. Phys. Lett.* **1984**, *111*, 326. Greene, B. I.; Hochstrasser, R. M.; Weisman, R. B. *Chem. Phys. Lett.* **1979**, *62*, 427. Chang, T.-C.; Dlott, D. D. *J. Chem. Phys.* **1989**, *90*, 3590. Laermer, F.; Elsaesser, T.; Kaiser, W. *Chem. Phys. Lett.* **1989**, *156*, 381. Heilweil, E. J.; Doany, F. E.; Moore, R.; Hochstrasser, R. M. *J. Chem. Phys.* **1982**, *76*, 532. Wondrazek, F.; Seilmeier, A.; Kaiser, W. *Chem. Phys. Lett.* **1984**, *104*, 121. Laubereau, A.; Kaiser, W. *Rev. Mod. Phys.* **1978**, *50*, 607.

(20) Henry, E. R.; Eaton, W. A.; Hochstrasser, R. M. *Proc. Natl. Acad. Sci. U.S.A.* **1986**, *83*, 8982.

(21) Genberg, L.; Richard, L.; McLendon, G.; Miller, R. J. D. *Science* **1991**, *251*, 1051. Genberg, L.; Heisel, F.; McLendon, G.; Miller, R. J. D. *J. Phys. Chem.* **1987**, *91*, 5521.

~10 ns excitation pulses. At the lowest flux (<0.1 × 10^7 W/cm^2), the anti-Stokes/Stokes intensity ratios for the A_{1g} modes ν_4 and ν_7 were found to be consistent with a heme at thermal equilibrium at or near room temperature. As the laser flux was increased, however, the Raman scattering no longer reflected an statistical distribution of vibrational energy. At the highest flux (~10 × 10^7 W/cm^2), the behavior of the ν_4 Stokes and anti-Stokes scattering indicated a heme at ~600 K, while ν_7 appeared much cooler at ~415 K.

This flux-mediated transition from a thermal to a nonthermal heme also was apparent in the band features of the ν_4 and ν_7 Stokes and anti-Stokes transitions in the nanosecond TRR spectra. Initially, the anti-Stokes widths and positions were very similar to their Stokes counterparts for both modes. As the incident flux of the nanosecond pulses increased, this behavior was retained by the ν_7 mode. However, the band shape and position of the anti-Stokes scattering from ν_4 systematically varied as it gained intensity. The ν_4 anti-Stokes signal symmetrically broadened by up to ~10 cm^{-1} and shifted to lower frequency by as much as 7 cm^{-1} relative to the corresponding Stokes line. These results support the conclusion derived from the flux-dependence of the anti-Stokes/Stokes area ratios. The ν_4 mode appears to retain significantly more vibrational energy than does ν_7.

The results presented here extend the nanosecond TRR studies into the picosecond temporal domain and to higher photon densities. While the nanosecond and picosecond TRR results are complementary, care must be exercised in their comparison. In the nanosecond TRRS experiments, the pulses were of sufficient duration to permit the establishment of a true steady-state vibrational energy distribution. On the other hand, a temporal pulse width of ~35 ps does not allow the system to attain a steady state. Hence, the picosecond TRRS experiments probed populations that were in flux. In addition, though the *peak* powers were higher in the 35 ps pulses, about 2 orders of magnitude more *total* energy was deposited in the system with each 10 ns pulse. With these issues in mind, comparisons of the picosecond TRRS and nanosecond TRRS results permit several valuable qualitative conclusions to be drawn about the mode selectivity of the vibrational energy dynamics associated with the ground state of iron porphyrins.

The behavior of the ν_4 and ν_7 Stokes and anti-Stokes scattering in the picosecond TRR studies is entirely consistent with the conclusions formed from the previous nanosecond experiments, and with results from earlier picosecond TRR studies of ν_7 carried out by Alden et al.[14a] The anti-Stokes/Stokes ratios showed a nonthermal vibrational energy distribution of the heme at all laser intensities employed. At the highest flux (~12 × 10^8 W/cm^2), the ν_4 mode was found to contain significantly more energy than did ν_7. The anti-Stokes/Stokes ratio for the ground state ν_4 scattering reflects a heme "temperature" of 820 K. A 4-fold decrease in laser flux resulted in a "temperature" of about 240 K lower. By comparison, over the same flux range, the ν_7 anti-Stokes/Stokes ratio reflected a significantly lower heme "temperature" of ~300 K, and the change in "temperature" was only 30 K. This low "temperature" associated with ν_7 was also observed in earlier studies by Ondrias, Friedman, and co-workers.[14a]

While these intensity ratios are qualitatively similar to those found in the nanosecond TRR studies, there also are some important differences. The ν_4 mode gets significantly "hotter" in the picosecond TRR studies, and the anti-Stokes/Stokes ratio is more sensitive to changes in the incident laser flux. In contrast, the ν_7 behavior in the picosecond TRR experiments reflects a "cooler" heme than is found in the nanosecond TRR studies. The relative insensitivity of the degree of excitation of this mode to the incident flux is comparable in the picosecond and nanosecond TRR studies, however. These observations lead to the following conclusions about the origin of the mode selectivity in the vibrational energy distribution in photoexcited hemes.

There are several phenomena that could be responsible for the mode selectivity observed in the vibrational energy distribution in this system. The heme undergoes four different types of processes within the duration of the incident pulses: (1) photoexcitation to the Soret excited electronic state, (2) nonradiative decay through *at least* one intermediate excited electronic state and then to the ground electronic state, (3) intramolecular vibrational energy redistribution (IVR), and (4) intermolecular vibrational energy relaxation (VR).

The first step in the heme photodynamic cycle certainly is mode selective. Vibrational degrees of freedom couple to the electromagnetic field with varying abilities. Raman excitation profiles have shown that the two A_{1g} modes examined in this study, ν_4 and ν_7, both couple quite strongly to the incident field and with comparable efficiencies.[22] In fact, in ferrocytochrome *c*, ν_7 has about twice the linear coupling strength as does ν_4. Both of these modes are likely to acquire considerable excitation in the initial photoinduced step, and hence, this process is probably not the origin of the mode selectivity observed in subsequent states.

Little is known about the details of the nonradiative decay steps. Issues concerning mode selectivity, for example, remain largely unresolved. Some general comments and estimates can be made, however. It is likely that intra- and intermolecular vibrational energy redistribution processes cannot compete with the very rapid (τ < 50 fs, $\tau_I \approx$ 300 fs) nonradiative steps. Although specific details about the electronic decay kinetics could not be measured in the picosecond TRR studies, Petrich et al.[8] determined that ~65% of the initial excitation of an unligated heme in deoxymyoglobin decays as Hb_I*. It seems reasonable, then, to estimate that more than half of the hemes photoexcited within the 35 ps pulses used in the picosecond TRR experiments return to the electronic ground state within 500 fs. The vibrational energy distribution of this ground electronic state then probably reflects that of the initial photoexcited state, in which both ν_4 and ν_7 have considerable population. The minor nonradiative decay pathway may lead to a different initial ground state vibrational energy distribution, as IVR is likely to temporally overlap this ~3 ps process. With these estimates, it is reasonable to conclude that the *initial* vibrational energy distribution in the ground state heme has significant population in ν_4 and ν_7. The mode selectivity thus appears to arise, at least in part, in IVR and VR associated with the ground electronic state.

The ν_7 anti-Stokes/Stokes intensity ratios in the picosecond and nanosecond TRRS experiments indicate that this mode couples quite well to its environment. This mode apparently readily loses its excess vibrational energy and very rapidly reflects the environmental temperature. This explains the counterintuitive behavior of this mode, in which a lower ν_7 "temperature" is observed in the picosecond TRR experiments relative to that in the nanosecond TRR experiments. A 10 ns laser pulse deposits a significant amount of total energy in the system. Each molecule in the illuminated volume is exposed to 50−500 photons per pulse. The system can thus accumulate significant energy in the local heme bath. The picosecond pulses are of higher peak intensity but are much shorter in duration (approximately 2−5 photons per molecule per pulse). Thus, the sample absorbs less total energy from a 35 ps pulse than

(22) Shomaker, K. T.; Champion, P. M. *J. Chem. Phys.* **1986**, *84*, 5314.

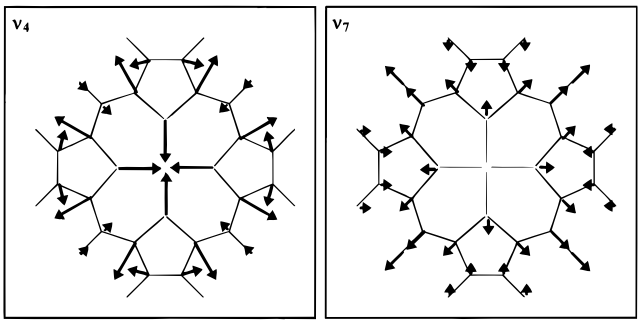

Figure 6. Normal coordinate displacement vectors of nickel octaethylporphyrin. The lengths of the vectors correspond qualitatively to the displacement magnitudes. Adapted from ref 23.

from a 10 ns pulse, and local heating should be significantly reduced. The relative insensitivity of the population of ν_7 to changes in excitation flux also is consistent with the hypothesis that ν_7 reflects the local bath temperature. The degree of excitation of the local solvent should not be very sensitive to incident flux, as the excess vibrational energy has many degrees of freedom among which to disperse.

The behavior of ν_4, however, indicates that this vibrational mode acts as a bottleneck in vibrational energy redistribution and relaxation. This mode apparently does not couple well to either the heat reservoir or to the ν_7 vibration at any excitation levels employed. The anti-Stokes/Stokes area ratio consistently reflects a ν_4 vibrational manifold that is more excited than the bath temperature indicated by ν_7. In addition, the anti-Stokes/Stokes area ratio is much more sensitive to laser flux when picosecond rather than nanosecond pulses are used. Excess vibrational energy deposited in the ν_4 degree of freedom does not dissipate efficiently on a 1−10 ps time scale. We conclude that the flux sensitivity of ν_4 reflects the reduced coupling of this mode to the bath and to the rest of the porphyrin, thereby allowing small amounts of energy to raise and maintain the "temperature" of this degree of freedom quite efficiently.

It is important to consider whether the preferential retention of vibrational energy in ν_4 is intrinsic to the metalloporphyrin or derives from its interactions with its protein environment. This question was addressed by earlier nanosecond TRRS studies carried out upon iron porphyrin model compounds in two very different solvent environments: Fe^{II} protoporphyrin IX−2-methylimidazole in detergent micelles[15] and Fe^{II} octaethylporphyrin−2-methyl imidazole in CH_2Cl_2.[17] In both of these systems, *qualitatively* similar results to those found for dHb were obtained. The ν_4 mode selectively retained vibrational energy derived from photoexcitation while ν_7 did not. Thus, while the magnitude of the effect may be influenced by the environment, the bottleneck character of the ν_4 mode appears to be intrinsic to the metalloporphyrin.

At this point, although it is clear that the observed mode selective behavior is intrinsic to the metalloporphyrin, insufficient information is available to allow meaningful conclusions to be drawn concerning the origin of the different vibrational behavior exhibited by ν_4 and ν_7. Both modes are delocalized and have A_{1g} symmetry (Figure 6). The ν_4 mode contains significant pyrrole ring breathing, while breathing of the 16-atom inner macrocycle makes up ν_7.[23] The ν_7 vibration also contains much more methine bridge motion than does ν_4. We speculate that because of the relatively isolated pyrrole motions associated with ν_4 this mode may be more local in nature. However, no conclusions concerning the differing abilities of these vibrations to couple to the bath are obvious from this inspection of the normal mode displacement vectors.

It is clear that the ν_4 coordinate has considerable anharmonic character. The anti-Stokes ν_4 transition shifts significantly to lower frequency as higher levels in the manifold are populated. In addition, measurements of the first overtone for this mode indicate a 2−3 cm^{-1} difference between the 0−1 and 1−2 transition energies (data not shown). However, the data presented here suggest that this mode couples poorly to both the bath and the rest of the molecule. These observations indicate that the anharmonicity in ν_4 arises from diagonal elements in the potential (i.e., $(\partial^3 H_{el}/\partial Q_J^3)_0 Q_J^3$ and higher order terms) rather than from off-diagonal elements, such as $(\partial^3 H_{el}/\partial Q_J \partial Q_K \partial Q_L)_0 Q_J Q_K Q_L$, that would allow coupling to other heme vibrational degrees of freedom. While this conclusion is quite interesting, it does not shed much light upon the basis for the vibrational bottleneck behavior of ν_4. Further studies will directly address these issues.

Summary

We report upon the use of picosecond transient vibrational spectroscopy to explore the vibrational dynamics of the electronic ground state of the heme active site of dHb. A model has been developed that unifies the previous observations of several research groups and strongly supports the conclusion that the flux-dependent, mode selective anti-Stokes behavior observed in this system has its origin in vibrational dynamics, rather than in electronic excited state populations.

This study confirms and extends previous observations that vibrational dynamics of the heme active site of dHb are quite mode specific. The ν_7 mode appears to couple efficiently to other degrees of freedom in this system. Excess vibrational energy placed in this mode rapidly disperses to the local environment. Hence, the excitation behavior of ν_7 reflects a mode in rapid thermal equilibrium with its surroundings. The higher frequency mode ν_4, on the other hand, does not appear to couple well to either ν_7 or to other vibrational degrees of freedom. Excess energy placed in this modes does not rapidly dissipate. Thus, the ν_4 mode acts as a vibrational bottleneck.

The results presented here indicate that vibrational energy redistribution and relaxation can play significant roles in the dynamics of large molecules on time scales as long as several picoseconds. These findings naturally lend themselves to speculation concerning the potential functional ramifications of vibrational energy bottlenecks in large molecules in condensed phase.

Acknowledgment. M. C. Simpson was formerly M. C. Schneebeck. M.R.O. acknowledges support from the NIH (GM33330). J.M.F. acknowledges support from the NIH (GM44343) and the W. M. Keck Foundation. M.C.S. acknowledges the support of the Howard Hughes Predoctoral Fellowship Program and the Department of Energy Distinguished Postdoctoral Research Program and helpful conversations with Erik Deumens.

JA961198J

(23) Abe, M.; Kitigawa, T.; Kyogoku, Y. *J. Chem. Phys.* **1978**, *69*, 4526.